

## ORIGINAL ARTICLE

# Critical role of fractalkine (CX<sub>3</sub>CL1) in cigarette smoke-induced mononuclear cell adhesion to the arterial endothelium

Cristina Rius,<sup>1,2</sup> Chantal Company,<sup>1,2</sup> Laura Piqueras,<sup>2</sup> Jose Miguel Cerdá-Nicolás,<sup>2,3</sup> Cruz González,<sup>2,4</sup> Emilio Servera,<sup>2,4</sup> Andreas Ludwig,<sup>5</sup> Esteban J Morcillo,<sup>1,2,6</sup> Maria-Jesus Sanz<sup>1,2</sup>

► Additional data are published online only. To view these files please visit the journal online (<http://dx.doi.org/10.1136/thoraxjnl-2012-202212>)

<sup>1</sup>Department of Pharmacology, Faculty of Medicine, University of Valencia, Valencia, Spain

<sup>2</sup>Institute of Health Research-INCLIVA, Valencia, Spain

<sup>3</sup>Department of Pathology, Faculty of Medicine, University of Valencia, Valencia, Spain

<sup>4</sup>Neumology Unit, University Clinic Hospital of Valencia (INCLIVA), University of Valencia, Valencia, Spain

<sup>5</sup>Institute of Pharmacology and Toxicology RWTH, Aachen University, Aachen, Germany

<sup>6</sup>Ciber CB06/06/0027 'Respiratory Diseases', Carlos III Health Institute, Spanish Ministry of Health, Spain

## Correspondence to

Dr Maria-Jesus Sanz, Department of Pharmacology, University of Valencia, 46010 Valencia, Spain; [maria.j.sanz@uv.es](mailto:maria.j.sanz@uv.es)

Received 29 May 2012

Revised 4 October 2012

Accepted 12 October 2012

Published Online First

9 November 2012

## ABSTRACT

**Background** Cigarette smoking is an important risk factor for the development of cardiovascular disease, yet the pathways through which this may operate are poorly understood. Therefore, the mechanism underlying cigarette smoke (CS)-induced arterial endothelial dysfunction and the potential link with fractalkine/CX<sub>3</sub>CL1 upregulation were investigated.

**Methods and results** Stimulation of human arterial umbilical endothelial cells (HUAECs) with pathophysiological concentrations of CS extract (1% CSE) increased CX<sub>3</sub>CL1 expression. Neutralisation of CX<sub>3</sub>CL1 activity under dynamic flow conditions significantly inhibited CSE-induced mononuclear cell adhesion to HUAECs (67%). The use of small interfering RNA (siRNA) revealed that nicotinamide adenine dinucleotide phosphate (NADPH) oxidase 5 (Nox5) but not Nox2 or Nox4 is the main NADPH isoform involved in CSE-induced CX<sub>3</sub>CL1 upregulation and mononuclear cell arrest. Knock down of HUAEC tumour necrosis factor  $\alpha$  expression with siRNA or pharmacological inhibition of p38 mitogen-activated protein kinase and nuclear factor  $\kappa$ B also abolished these responses. Interestingly, circulating monocytes and lymphocytes from patients with chronic obstructive pulmonary disease (COPD) (n=29) versus age-matched controls (n=23) showed CX<sub>3</sub>CR1 overexpression. Furthermore, CX<sub>3</sub>CL1 neutralisation dramatically diminished their enhanced adhesiveness to CSE-stimulated HUAECs. Finally, when animals were exposed for 3 days to CS, a mild inflammatory response in the lung was observed which was accompanied by enhanced CX<sub>3</sub>CL1 expression in the cremasteric arterioles, an organ distant from the lung. CS exposure resulted in increased leukocyte-arteriolar endothelial cell adhesion which was significantly reduced (51%) in animals lacking CX<sub>3</sub>CL1 receptor (CX<sub>3</sub>CR1).

**Conclusions** These results suggest that CS induces functional CX<sub>3</sub>CL1 expression in arterial endothelium and leukocytes from patients with COPD show increased CX<sub>3</sub>CL1-dependent adhesiveness. Therefore, targeting the CX<sub>3</sub>CL1/CX<sub>3</sub>CR1 axis might prevent COPD-associated cardiovascular disorders.

## INTRODUCTION

Chronic obstructive pulmonary disease (COPD) is characterised by a progressive and largely irreversible decrement in lung function associated with an

## Key messages

### What is the key question?

- How does cigarette smoke (CS) induce arterial endothelial dysfunction and leukocyte recruitment?

### What is the bottom line?

- Fractalkine/CX<sub>3</sub>CL1 is upregulated in the arterial endothelium after stimulation with CS extract, increasing the endothelial adhesiveness for CX<sub>3</sub>CL1 receptor (CX<sub>3</sub>CR1)-expressing cells. Blockade of the CX<sub>3</sub>CL1/CX<sub>3</sub>CR1 axis dramatically reduced the arterial adhesion of mononuclear leukocytes from patients with chronic obstructive pulmonary disease (COPD) to CS extract-stimulated endothelium.

### Why read on?

- This is the first report that has systematically characterised the underlying mechanisms involved in CS-induced arterial endothelial dysfunction. We have provided evidence that CX<sub>3</sub>CL1 upregulation is a critical molecule in CS-induced mononuclear leukocyte recruitment. Therefore, CX<sub>3</sub>CL1 and CX<sub>3</sub>CR1 may be considered as potential drug targets for the prevention and treatment of COPD-associated cardiovascular disorders.

abnormal chronic inflammatory response of the lungs to noxious particles and gases, mostly from cigarette smoke (CS).<sup>1</sup> In addition to the pulmonary features of COPD, several systemic effects have been recognised, such as skeletal muscle dysfunction, cardiovascular disease, osteoporosis and diabetes.<sup>1</sup> Epidemiological studies demonstrate that smoking is a significant risk factor for heart disease, including aneurysm formation and rupture, stroke and atherosclerosis,<sup>2</sup> which is one of the leading causes of morbidity and mortality in Western countries.<sup>3</sup> One of the earliest stages of atherogenesis is endothelial dysfunction, which leads to a proinflammatory and prothrombotic phenotype of the endothelium<sup>4</sup> and thus provokes the attachment and the subsequent migration of leukocytes. In this context, vascular dysfunction in smokers has been widely described.<sup>5,6</sup>

**To cite:** Rius C, Company C, Piqueras L, et al. *Thorax* 2013;**68**:177–186.

Adhesive interactions between leukocytes and arterial endothelium precede leukocyte infiltration to the subendothelial space.<sup>7</sup> The migration of leukocytes from the blood to sites of extravascular injury is mediated through a sequential cascade of leukocyte–endothelial cell adhesive interactions which involve an array of cell adhesion molecules (CAMs) present on leukocytes and endothelial cells.<sup>7</sup> In addition to CAMs, chemokines have the potential to recruit specific cell types and are involved in the regulation of leukocyte trafficking.<sup>8</sup> Fractalkine (CX<sub>3</sub>CL1) is the unique member of the CX<sub>3</sub>C subfamily and is expressed in a soluble and membrane-bound form on the surface of inflamed endothelium. As a full-length transmembrane protein, CX<sub>3</sub>CL1 acts as an adhesion molecule.<sup>9</sup> Cleavage of the CX<sub>3</sub>CL1 mucin stalk close to the junction with the transmembrane domain produces a soluble form of CX<sub>3</sub>CL1 that is a potent chemoattractant for monocytes and T cells but not for neutrophils.<sup>10</sup> It interacts with leukocytes expressing its receptor CX<sub>3</sub>CR1. The ability of fractalkine to attract and arrest blood monocytes and lymphocytes, and its presence in vascular wall cells makes it an attractive candidate for playing a pivotal role in atherosclerotic lesion formation. Indeed, independent studies with CX<sub>3</sub>CR1<sup>-/-</sup> apolipoprotein E<sup>-/-</sup> or CX<sub>3</sub>CR1<sup>-/-</sup> LDLr<sup>-/-</sup> mice have associated a substantial decrease in macrophage infiltration within the arterial wall with a marked reduction in atherosclerosis development, suggesting a relevant role for the CX<sub>3</sub>CL1/CX<sub>3</sub>CR1 axis.<sup>11 12</sup>

The mechanisms by which CS promotes the development of a proinflammatory environment in the vessel wall are not fully understood and experimental data evaluating the impact of CS within the cardiovascular system using *in vitro* and *in vivo* approaches are scarce. Therefore, in this study we sought to determine whether CS induces functional CX<sub>3</sub>CL1 expression in organs distant from the lung and the underlying mechanisms involved in these responses. *In vitro* experiments were carried out in primary cultures of human arterial endothelial cells stimulated with CS extract (CSE). Additionally, to explore the clinical consequences of our findings, CX<sub>3</sub>CR1 receptor expression in different circulating leukocyte subsets from patients with chronic obstructive pulmonary disease was analysed and their CX<sub>3</sub>CR1-dependent adhesiveness to human umbilical arterial endothelial cells (HUAECs) evaluated. Finally, intravital microscopy within the murine cremasteric microcirculation was used to determine leukocyte–endothelial cell interactions induced by CS exposure.

## METHODS

### Human *in vitro* studies

All investigation with human samples carried out in the present study conforms with the principles outlined in the Declaration of Helsinki and was approved by the institutional ethics committee at the University Clinic Hospital of Valencia, Spain. Written informed consent was obtained from all volunteers.

### CSE preparation

Cigarettes were obtained from the Kentucky Tobacco Research and Development Center at the University of Kentucky. CSE was prepared as described previously.<sup>13</sup> Further details are described in the online data supplement.

### Reverse transcriptase PCR

Total RNA was isolated from cultured HUAECs by using Trizol Isolation Reagent. Details are found in the online data supplement.

### Flow cytometry

After treatments, endothelial cells were detached from culture flasks by treatment with ice-cold phosphate-buffered saline containing 0.05% NaN<sub>3</sub> and 0.2% bovine serum albumin, subsequent scraping and centrifugation. Details are described in the online data supplement.

### Leukocyte–endothelial cell interactions under flow conditions

HUAECs were grown to confluence and subjected to different treatments. Further details are found in the online data supplement.

### Immunofluorescence

CX<sub>3</sub>CL1 expression was visualised in HUAECs by indirect immunofluorescence. Details are described in the online data supplement.

### Western blot

CX<sub>3</sub>CL1 expression was also determined by immunoblotting. Further details are provided in the online data supplement.

### Transfection of tumour necrosis factor $\alpha$ , Nox2, Nox4 or Nox5 small interfering RNA

Endothelial cell gene silencing was performed using either control or tumour necrosis factor  $\alpha$  (TNF $\alpha$ ), nicotinamide adenine dinucleotide phosphate (NADPH) oxidase 2 (Nox2), Nox4 or Nox5-specific small interfering RNA. Details are described in the online data supplement.

### Experimental protocols

Details of all the experimental protocols followed in this study are provided in the online data supplement.

### Studies in patients with COPD and age-matched controls

Patients' details, the procedure for determining CX<sub>3</sub>CR1 expression on circulating leukocytes, their adhesiveness to CSE-stimulated HUAECs and plasma CX<sub>3</sub>CL1 levels can be found in the online data supplement.

### *In vivo* animal studies

#### CS exposure

Exposure of mice to CS was carried out using a modified method previously described.<sup>14</sup> Details of the procedure are found in the online data supplement.

#### Intravital microscopy

Intravital microscopy was carried out in the mouse cremasteric microcirculation. Details of the technique are provided in the online data supplement.

#### Histology and immunohistochemistry

Immunofluorescence studies were performed in the cremasteric microvasculature. Details of the procedure are found in the online data supplement.

### Materials

All materials used are listed in the online data supplement.

### Statistical analysis

The statistical analyses used are provided in the online data supplement.

## RESULTS

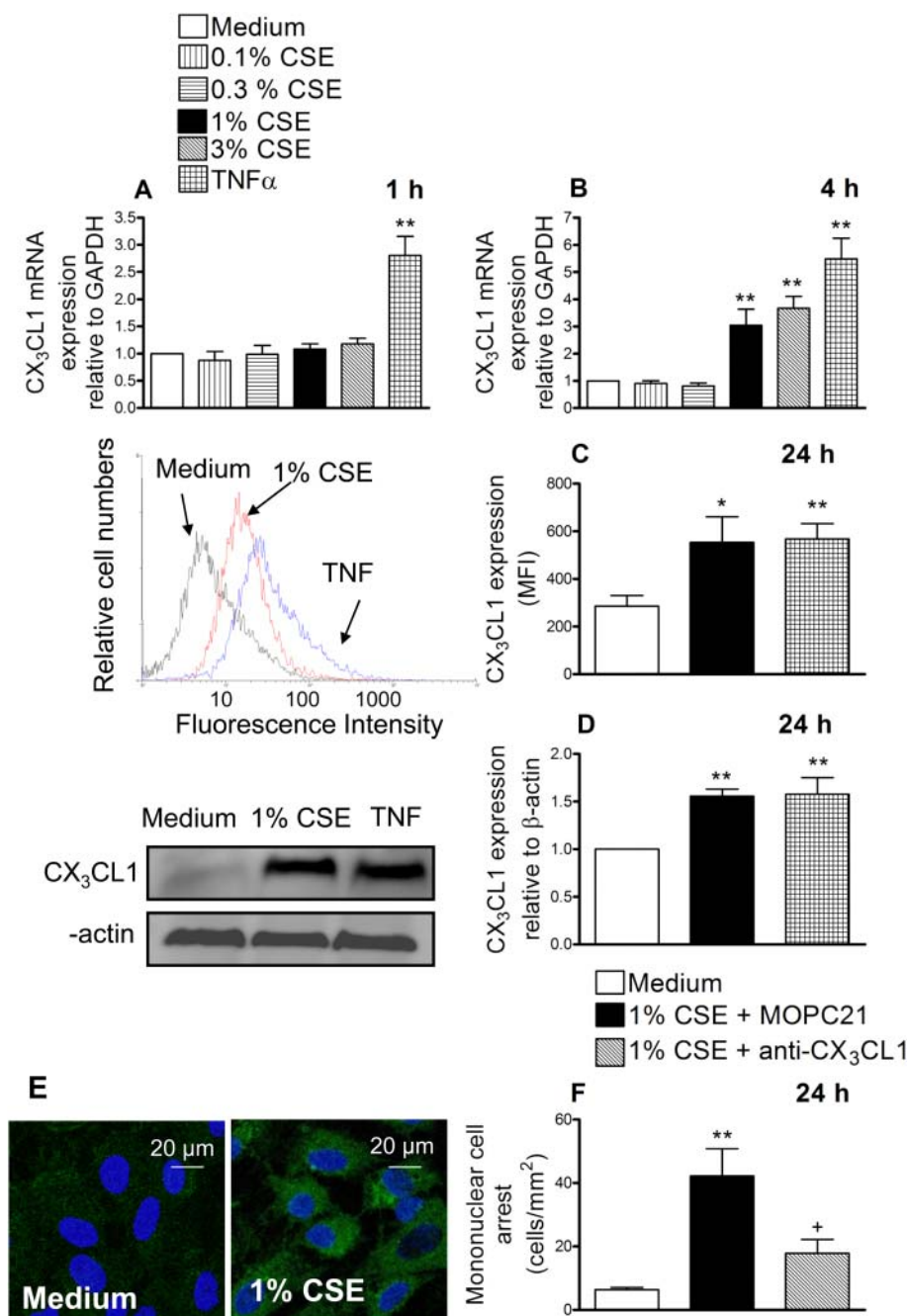
CSE induces functional CX<sub>3</sub>CL1 expression in HUAECs

HUAECs were incubated with different CSE concentrations (0.1%–3%) or TNF $\alpha$  (20 ng/ml) for 1 or 4 h. Reverse transcriptase PCR revealed that after 1 h of incubation with CSE no changes in CX<sub>3</sub>CL1 mRNA expression were detected whereas TNF $\alpha$  provoked a clear enhancement (figure 1A). When cells were stimulated with CSE for 4 h, a concentration-dependent increase in CX<sub>3</sub>CL1 mRNA expression was observed (figure 1B). Based on these results, the concentration of 1% CSE was used for the remainder experiments. This concentration approximately

corresponds to exposures associated with smoking 1.5 packs per day as previously estimated<sup>15</sup> and it is consistent with the amount smoked by the patients with COPD used in this study. In addition, it did not cause cytotoxicity to endothelial cells as found with the 3% CSE concentration (assessed by MTT and lactate dehydrogenase release assays, data not shown).

Therefore, we next evaluated the effect of CSE at the protein level. Endothelial cells were stimulated with 1% CSE for 24 h and analysed by flow cytometry. CX<sub>3</sub>CL1 expression was detected in CSE-stimulated HUAECs (figure 1C). We further confirmed these observations by western blot (figure 1D) and immunofluorescence

**Figure 1** Cigarette smoke extract (CSE) induces CX<sub>3</sub>CL1 mRNA and protein expression in human arterial umbilical endothelial cells (HUAECs) (A–E). A neutralising antibody against CX<sub>3</sub>CL1 function inhibited the recruitment of mononuclear leukocytes to CSE-stimulated HUAECs (F). HUAECs were stimulated with CSE (0.1–3%) or tumour necrosis factor  $\alpha$  (TNF  $\alpha$ ) (20 ng/ml) for 1, 4 or 24 h. Relative quantification of mRNA levels for CX<sub>3</sub>CL1 and glyceraldehyde 3-phosphate dehydrogenase (GAPDH) was determined by using reverse transcriptase PCR by the comparative Ct method ( $\Delta\Delta C_t$  method). Columns show the fold increase in expression of CX<sub>3</sub>CL1 mRNA, relative to control GAPDH values, calculated as mean $\pm$ SEM of the  $2^{-\Delta\Delta C_t}$  values (n=3–4 independent experiments). Protein expression was determined by flow cytometry and expressed as mean fluorescence intensity (MFI). Representative histograms are also shown (mean $\pm$ SEM of n=7 independent experiments). Following a similar protocol, CX<sub>3</sub>CL1 expression was also determined by western blotting. Results (mean $\pm$ SEM of n=5–6 independent experiments) are expressed as fold increase in CX<sub>3</sub>CL1: $\beta$  actin. Representative gels are shown above. \*p<0.05 or \*\*p<0.01 relative to values in the medium group. CX<sub>3</sub>CL1 upregulation was visualised in non-permeabilised HUAECs by immunofluorescence (green). Nuclei were counterstained with 4'6-diamidino-2-phenylindole (DAPI). Results are representative of n=5 independent experiments. Endothelial cells were stimulated with 1% CSE for 24 h. Some cells were incubated with a neutralising antibody against CX<sub>3</sub>CL1 function (5  $\mu$ g/ml) or with an irrelevant isotype-matched monoclonal antibody (MOPC21, 5  $\mu$ g/ml). Then human mononuclear cells ( $1 \times 10^6$  cells/ml) were perfused over the monolayers for 5 min at 0.5 dyn/cm<sup>2</sup> and leukocyte accumulation quantified. Results are the mean $\pm$ SEM of n=7 independent experiments. \*p<0.05 or \*\*p<0.01 relative to values in the medium group; +p<0.05 relative to 1% CSE group.



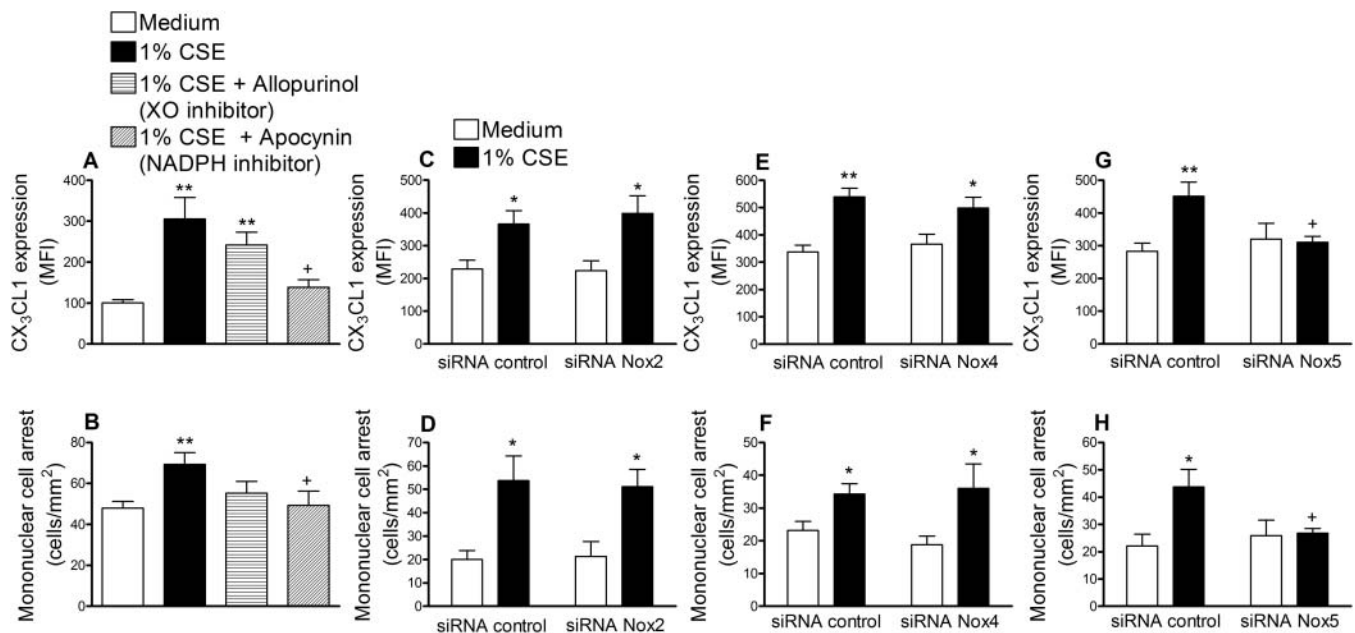


**Figure 2** Cigarette smoke extract (CSE)-induced CX<sub>3</sub>CL1 expression (A) and mononuclear cell arrest (B) is inhibited by apocynin but not by allopurinol. Nicotinamide adenine dinucleotide phosphate (NADPH) oxidase 5 (Nox5) but not Nox2 or Nox4 small interfering RNA (siRNA) inhibits CSE-induced CX<sub>3</sub>CL1 expression and mononuclear cell arrest in human arterial umbilical endothelial cells (HUAECs) (C–H). HUAECs were incubated with apocynin (30  $\mu$ M) or allopurinol (100  $\mu$ M) for 1 h and then stimulated with 1% CSE for 24 h. CX<sub>3</sub>CL1 expression was determined by flow cytometry. Results (mean $\pm$ SEM of n=6–7 independent experiments) are expressed as mean fluorescence intensity (MFI) (A). Human mononuclear cells ( $1 \times 10^6$  cells/litre) were perfused over the monolayers for 5 min at 0.5 dyn/cm<sup>2</sup> and leukocyte accumulation quantified (B). Results are the mean  $\pm$ SEM of n=6 independent experiments. \*\*p<0.01 relative to values in the medium group; +p<0.05 relative to 1% CSE group. Endothelial cells were transfected with Nox2, Nox4 or Nox5 siRNA or control siRNA. 48 h post-transfection cells were stimulated with 1% CSE for 24 h. CX<sub>3</sub>CL1 expression was determined by flow cytometry. Results (mean $\pm$ SEM of n=5–7 independent experiments) are expressed as MFI (C, E and G). \*p<0.05 or \*\*p<0.01 relative to values in the medium group; +p<0.05 relative to 1% CSE group in control siRNA transfected cells. Human mononuclear cells ( $1 \times 10^6$  cells/ml) were perfused over the monolayers for 5 min at 0.5 dyn/cm<sup>2</sup> and leukocyte accumulation quantified (D, F and H). Results are the mean $\pm$ SEM of n=5–7 independent experiments. \*p<0.05 or \*\*p<0.01 relative to values in the medium group; +p<0.05 relative to 1% CSE group in control siRNA transfected cells. XO, xanthine oxidase.

(figure 1E). To investigate the functional role of CSE-induced CX<sub>3</sub>CL1 expression, freshly isolated human mononuclear cells were perfused across a monolayer of HUAECs stimulated with 1% CSE for 24 h. As illustrated in figure 1F, significant increases in mononuclear cell arrest were observed in CSE-stimulated cells. Interestingly, neutralisation of CX<sub>3</sub>CL1 activity on the endothelial cell surface resulted in a significant reduction in CSE-induced mononuclear cell adhesion to HUAECs (67% inhibition), suggesting a potential role for this chemokine in the arterial mononuclear leukocyte recruitment associated with CS.

#### Nox5 but not Nox2 or Nox4 siRNA inhibits CSE-induced CX<sub>3</sub>CL1 expression and mononuclear cell arrest in HUAECs

CS-mediated oxidative stress is implicated in endothelial dysfunction and water-soluble components of CS smoke can increase reactive oxygen species (ROS) generation in endothelial cells.<sup>16</sup> Potential sources of superoxide anion in the vasculature include the activation of Noxs and xanthine oxidase (XO). Figure 2 illustrates that the inhibition of Nox with apocynin reduced CSE-induced CX<sub>3</sub>CL1 expression and mononuclear cell adhesion by 81% and 93% respectively. XO inhibition with allopurinol did not exert any significant inhibition.

Vascular Noxs are expressed in a cell-specific manner, with endothelial cells expressing mainly Nox2, Nox4 and Nox5.<sup>17 18</sup> To determine the Nox isoform implicated in CSE-induced responses, we used a siRNA approach for knocking down Nox2, Nox4 or Nox5 in HUAECs. Significant reductions in Nox2, Nox4 and Nox5 mRNA (71–80%) and CSE-induced

protein expression (60–68%) were evident after 48 h of incubation with their respective siRNA (see Figure I in online data supplement). Notably, whereas downregulation of Nox2 or Nox4 had no impact on CSE-induced CX<sub>3</sub>CL1 expression and mononuclear cell adhesion to HUAECs, Nox5 silencing dramatically inhibited these responses (figure 2G–H).

#### TNF $\alpha$ siRNA inhibits CSE-induced CX<sub>3</sub>CL1 expression and mononuclear cell arrest in HUAECs

Increased serum levels of TNF $\alpha$  have been detected in healthy smokers<sup>19</sup> and TNF $\alpha$  is one of the main inducers of CX<sub>3</sub>CL1 expression.<sup>9</sup> We first evaluated the effect of CSE on TNF $\alpha$  expression in HUAECs and increased expression was encountered after 24 h of stimulation (figure 3A). To suppress TNF $\alpha$  expression, again a siRNA approach was used. HUAECs showed a >80% reduction in TNF $\alpha$  mRNA and >70% decrease in the intracellular cytokine compared with control siRNA-treated cells (figure 3B and C). CSE extract significantly increased the expression of CX<sub>3</sub>CL1 and caused mononuclear cell recruitment in control siRNA-transfected cells (figure 3D and E). However, in TNF $\alpha$ -deficient HUAECs, CSE-induced responses were significantly reduced (figure 3D and E).

#### P38 mitogen-activated protein kinase and nuclear factor $\kappa$ B are involved in CSE-induced CX<sub>3</sub>CL1 expression and mononuclear cell arrest in HUAECs

Generation of oxidants by CS appears to be the primary stimulus for activation of mitogen-activated protein kinase (MAPK)

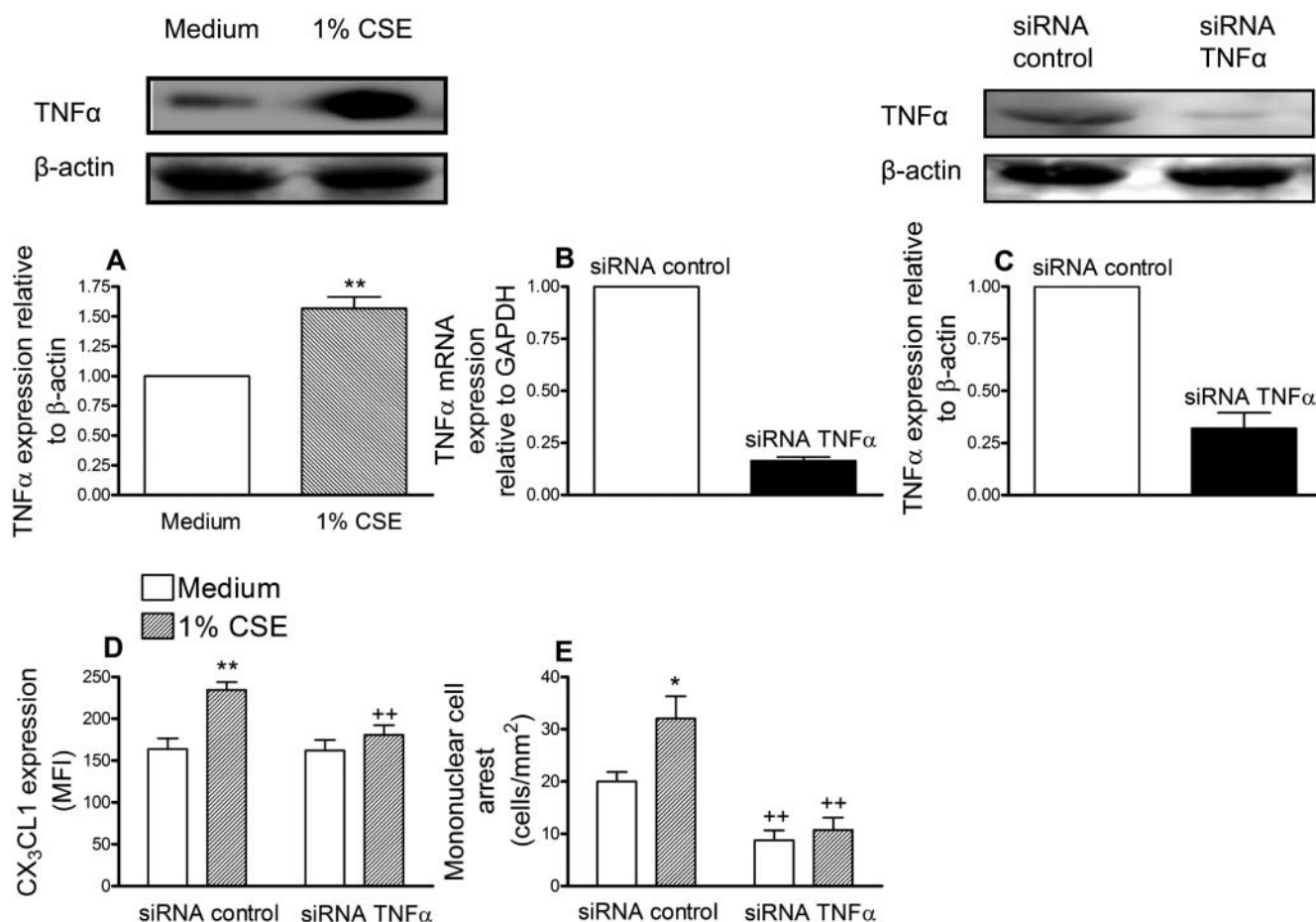


**Figure 3** Cigarette smoke extract (CSE) induces tumour necrosis factor  $\alpha$  (TNF $\alpha$ ) increased expression in human arterial umbilical endothelial cells (HUAECs) (A). TNF $\alpha$  small interfering RNA (siRNA) inhibits CSE-induced CX<sub>3</sub>CL1 expression (D) and mononuclear cell arrest (E) in HUAECs. HUAECs were stimulated with 1% CSE for 24 h. TNF $\alpha$  expression was determined by western blotting. Results (mean $\pm$ SEM of at least four independent experiments) are expressed as fold increase of the TNF $\alpha$ : $\beta$  actin. Representative gels are shown above. \*\* $p$ <0.01 relative to values in the medium group. Endothelial cells were transfected with TNF $\alpha$  siRNA or control siRNA. Knockdown of TNF $\alpha$  in HUAECs was determined by reverse transcriptase PCR (B) and western blotting (C). 48 h post transfection, cells were stimulated with 1% CSE for 24 h. CX<sub>3</sub>CL1 expression was determined by flow cytometry. Results (mean $\pm$ SEM of  $n=6$  independent experiments) are expressed as mean fluorescence intensity (MFI) (D). Human mononuclear cells ( $1 \times 10^6$  cells/ml) were perfused over the monolayers for 5 min at 0.5 dyn/cm<sup>2</sup> and leukocyte accumulation quantified (E). Results are the mean $\pm$ SEM of  $n=7-8$  independent experiments. \* $p$ <0.05 or \*\* $p$ <0.01 relative to values in the medium group; ++ $p$ <0.01 relative to their respective group in control siRNA transfected cells.

cascades at least in the lung epithelium.<sup>20</sup> In this study, CSE stimulation caused a rapid phosphorylation of p38 MAPK and the p65 subunit of nuclear factor  $\kappa$ B (NF $\kappa$ B) (figure 4A and B). Consequently, CSE-induced CX<sub>3</sub>CL1 expression and mononuclear cell adhesion were attenuated by pretreatment of the endothelial cells with the inhibitors of p38 MAPK or NF $\kappa$ B (figure 4C and D).

#### Circulating mononuclear cells from patients with COPD show increased fractalkine receptor expression (CX<sub>3</sub>CR1) and adhesiveness to CSE-stimulated HUAECs compared with those from healthy controls

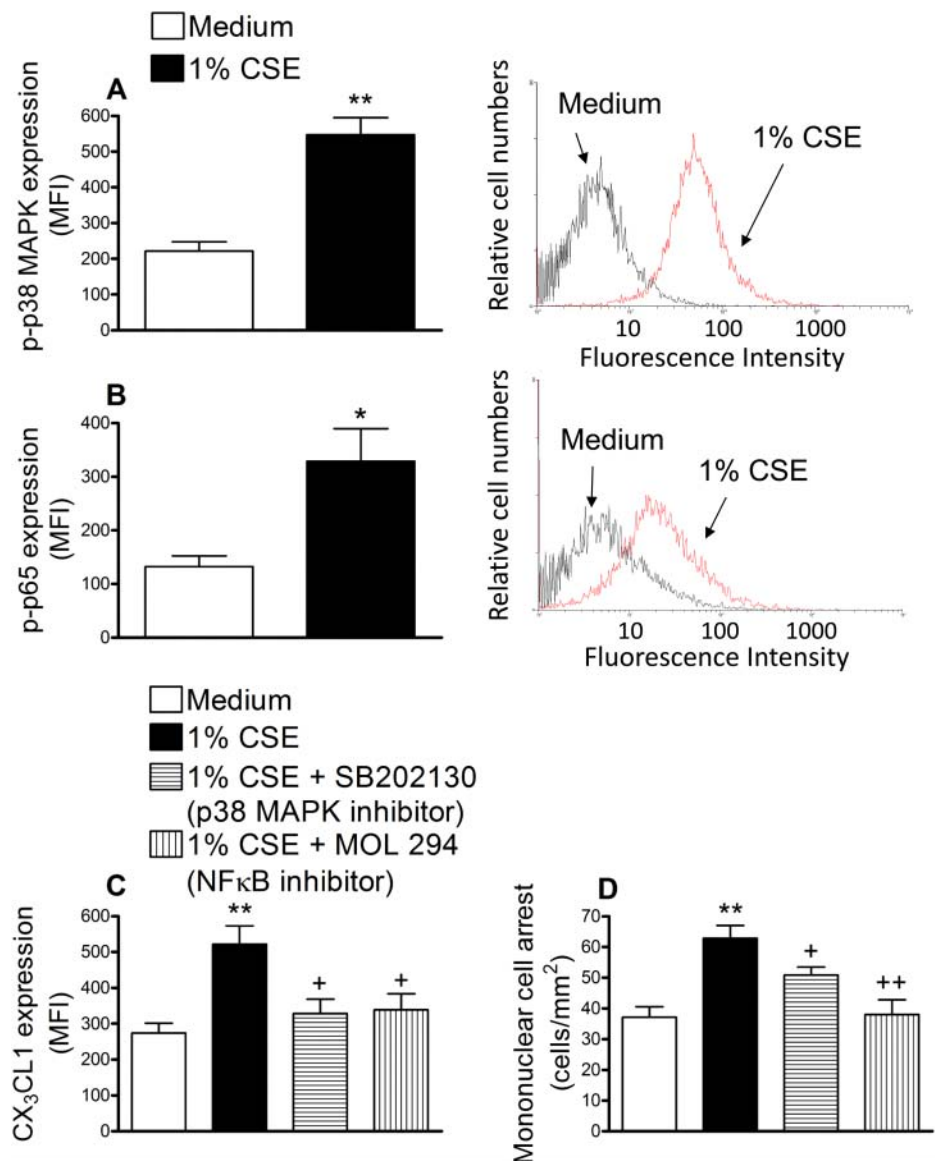
We next determined CX<sub>3</sub>CR1 expression on circulating monocytes and lymphocytes from patients with COPD and age-matched controls. As illustrated in figure 5A–D, increased and significant differences in CX<sub>3</sub>CR1 expression and the percentage of circulating leukocytes expressing it were detected in monocytes and lymphocytes from patients with COPD compared with those encountered in the control group. When whole blood from patients with COPD and their respective

controls was perfused across CSE-stimulated HUAECs, increased and significant differences in leukocyte adhesion were observed, being more marked in the COPD group (figure 5E). Neutralisation of CX<sub>3</sub>CL1 activity on endothelial cells resulted in a significant reduction in CSE-induced leukocyte adhesion (52% inhibition in the control group and 84% inhibition in the COPD group, figure 5E). Despite these findings, no significant differences in the circulating levels of soluble CX<sub>3</sub>CL1 were encountered between the groups investigated (figure 5F).

#### CS exposure induces lung inflammation and leukocyte–endothelial cell interactions in the mouse cremasteric microcirculation; arteriolar leukocyte adhesion was reduced in CX<sub>3</sub>CR1<sup>-/-</sup> mice

Finally, to explore the potential in vivo relevance of these findings, an acute model of CS exposure was used. Histological examination of the lungs of animals exposed to CS for 3 days revealed a clear inflammatory response (figure 6A). Although significant cell recruitment was found in CS-exposed animals, no differences in lung leukocyte numbers were encountered between

**Figure 4** Cigarette smoke extract (CSE) induces p38 mitogen-activated protein kinase (MAPK) (A) and nuclear factor  $\kappa$ B (NF $\kappa$ B) (B) activation in human arterial umbilical endothelial cells (HUAECs). CSE-induced CX<sub>3</sub>CL1 expression (C) and mononuclear cell arrest (D) in HUAECs is reduced by a p38 MAPK or a NF $\kappa$ B inhibitor. Cells were stimulated for 30 min or 1 h with 1% CSE. p38 MAPK and NF $\kappa$ B activation was determined by flow cytometry. Results (mean $\pm$ SEM of at least six independent experiments) are expressed as mean fluorescence intensity (MFI) (A and B). Representative histograms are also shown. \* $p$ <0.05 or \*\* $p$ <0.01 relative to values in the control group. HUAECs were incubated with SB202130 (20  $\mu$ M) or MOL294 (2.5  $\mu$ M) for 1 h and then stimulated with 1% CSE for 24 h. CX<sub>3</sub>CL1 expression was determined by flow cytometry. Results (mean $\pm$ SEM of  $n$ =6–7 independent experiments) are expressed as MFI (C). Human mononuclear cells ( $1 \times 10^6$  cells/ml) were perfused over the monolayers for 5 min at 0.5 dyn/cm<sup>2</sup> and leukocyte accumulation quantified (D). Results are the mean $\pm$ SEM of  $n$ =6–7 independent experiments. \*\* $p$ <0.01 relative to values in the medium group; + $p$ <0.05 or +++ $p$ <0.01 relative to 1% CSE group.



CX<sub>3</sub>CR1-expressing (CX<sub>3</sub>CR1<sup>+/+</sup>) and CX<sub>3</sub>CR1-deficient (CX<sub>3</sub>CR1<sup>-/-</sup>) mice (figure 6B). The recruited cells were mainly neutrophils (78.8 $\pm$ 2.9%) and mononuclear cell numbers remained unchanged. In addition, no significant increases in CX<sub>3</sub>CL1 mRNA expression were detected (figure 6D).

Intravital microscopy was used to examine the effect of CS exposure on leukocyte–endothelial cell interactions in an organ remote from the lung, the mouse cremasteric microcirculation. CS exposure induced a significant enhancement of arteriolar leukocyte adhesion in CX<sub>3</sub>CR1<sup>+/+</sup> and CX<sub>3</sub>CR1<sup>-/-</sup> mice (figure 6C) which was significantly reduced (51% inhibition) in CX<sub>3</sub>CR1-deficient mice (figure 6C). Mononuclear cells were found to be the cells primarily adhered to the CS-stimulated arterioles (86.6 $\pm$ 3.4%). While mRNA quantification and immunofluorescence analysis of the cremasteric microcirculation revealed that endothelial CX<sub>3</sub>CL1 expression was virtually absent in the cremasteric arterioles of mice not exposed to CS, increased chemokine mRNA and protein expression was found in the microvessels of those animals exposed to the stimulus (figure 6E and F).

## DISCUSSION

Cardiovascular diseases are more frequent and are found prematurely in patients with chronic inflammatory disorders such as COPD.<sup>1</sup> However, little is known regarding the mechanisms by which CS induces endothelial dysfunction in organs distant from the lung. In this study, we demonstrated for the first time that CSE induces CX<sub>3</sub>CL1-dependent mononuclear cell arrest in the arterial endothelium and unravels a previously undescribed mechanism by which CS affects arteriolar function in an adverse manner. Different human lymphocyte subsets as well as monocytes express CX<sub>3</sub>CR1 receptor,<sup>21</sup> which might explain the marked reduction in mononuclear cell adhesion to CSE-stimulated HUAECs after neutralising CX<sub>3</sub>CL1 activity.

Smoke-derived free radicals and oxidants are part of CS causing a pro-oxidative state in the circulatory system. CS exposure rapidly induces production of ROS impairing endothelial functions.<sup>22</sup> Moreover, CX<sub>3</sub>CL1 expression can be upregulated by oxidative stress<sup>23</sup> and we now report the involvement of ROS in CS-induced CX<sub>3</sub>CL1 expression and mononuclear leukocyte arrest since apocynin, an unspecific Nox inhibitor,

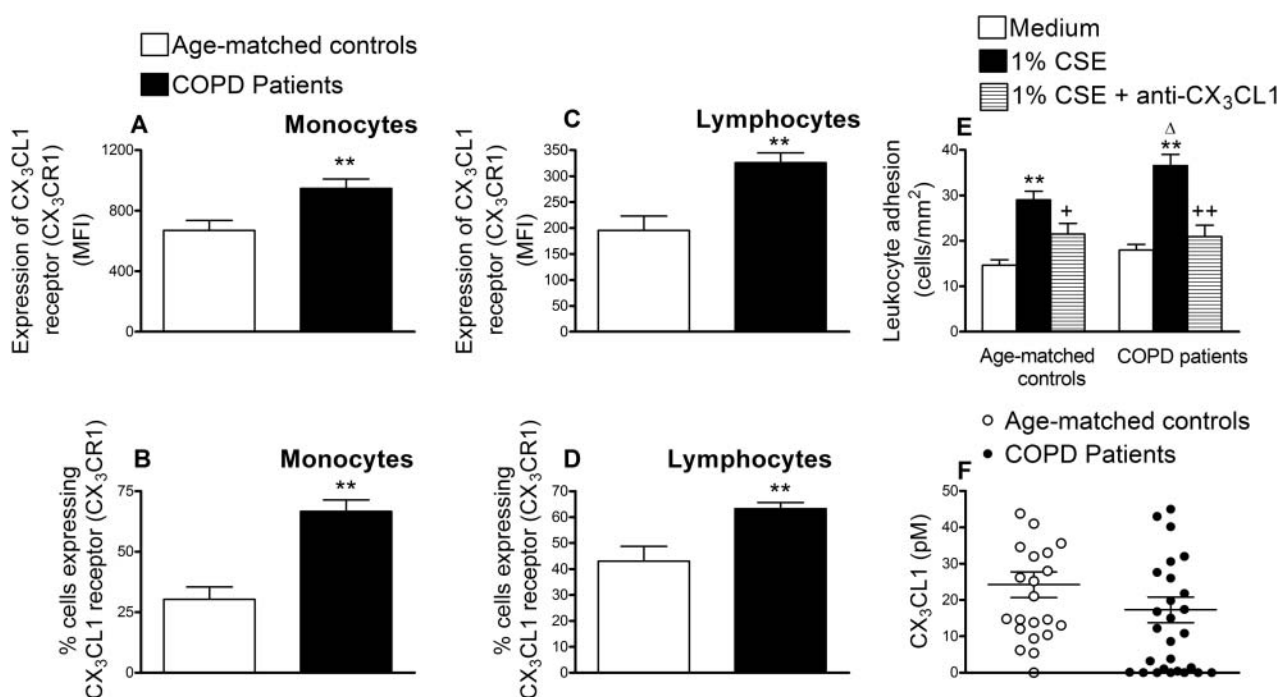


**Figure 5** CX<sub>3</sub>CL1 receptor expression (CX<sub>3</sub>CR1) in circulating monocytes and lymphocytes from patients with chronic obstructive pulmonary disease (COPD) and aged-matched controls (A–D), recruitment of leukocytes from whole blood of patients with COPD and aged-matched controls by cigarette smoke extract (CSE)-stimulated human arterial umbilical endothelial cells (HUAECs) (E) and CX<sub>3</sub>CL1 plasma levels in patients with COPD and aged-matched controls (F). Leukocytes were stained with a conjugated monoclonal antibody for CX<sub>3</sub>CR1 and analysed by flow cytometry (A–D). Results are mean ± SEM of n = 23–29 experiments and are expressed as mean fluorescence intensity and percentage of positive cells. \*\*p < 0.01 relative to values in the control group. HUAECs were stimulated with 1% CSE for 24 h. Some cells were incubated with a neutralising antibody against CX<sub>3</sub>CL1 function (5 μg/ml) or with an irrelevant isotype-matched monoclonal antibody (MOPC21, 5 μg/ml). Then, whole blood from patients with COPD and healthy aged-matched controls was perfused over the endothelial monolayers for 5 min at 0.5 dyn/cm<sup>2</sup> and leukocyte adhesion quantified (E). Results are the mean ± SEM of n = 20–22 experiments. \*p < 0.05 relative to values in the medium group. +p < 0.05 or ++p < 0.01 relative to 1% CSE group. Δ p < 0.05 relative to the values in the healthy aged-matched control group. CX<sub>3</sub>CL1 plasmatic levels were measured by ELISA (F). Results (pM in the plasma) are the mean ± SEM of n = 23–29 experiments.

diminished these responses. Based on these results, we tried to clarify the endothelial Nox isoforms involved in these findings. Endothelial cells mainly express Nox2, Nox4 and Nox5 isoforms<sup>17–18</sup> and while CSE stimulation of HUAECs caused increased Nox2 and Nox4 expression, their knockdown did not significantly impact CSE-induced responses. Conversely, Nox5 downregulation was able to abrogate CSE-induced CX<sub>3</sub>CL1 expression and subsequent mononuclear cell adhesion. Nevertheless, it cannot be excluded that the potential interaction of Nox5 with other Nox isoforms in the context of Nox5 downregulation, which may inhibit Nox5-associated Nox activity, although such contention requires further studies. Of note, a recent report has demonstrated the involvement of Nox5 in angiotensin-II-induced increased endothelial CAM expression,<sup>24</sup> a mediator that shares a similar profile of inflammatory effects with CS since both ROS generation and TNFα release seem to be involved in its proinflammatory activity.<sup>25–26</sup>

The role of TNFα in COPD is thought to be central to lung and systemic inflammation.<sup>1</sup> The potential implication of TNFα was investigated and CSE stimulation clearly increased the expression of this cytokine. We also revealed that TNFα silencing in HUAECs was associated with reductions in CSE-induced CX<sub>3</sub>CL1 expression with concomitant impairment in CSE-induced mononuclear leukocyte–endothelial cell interactions. Taken together, these findings suggest that CS contributes to endothelial dysfunction and vascular damage through TNFα release, which may exert autocrine/paracrine effects in the

arterial endothelium and probably in the vascular smooth muscle cells via increased CX<sub>3</sub>CL1 expression and subsequent leukocyte CX<sub>3</sub>CR1–endothelial CX<sub>3</sub>CL1 interactions.

Activation of MAPK signal transduction is important to stress-induced gene expression; such stresses include CS and TNFα.<sup>20</sup> We found that CSE-mediated activation of endothelial cells triggers different redox-sensitive signalling pathways likely activated by NADPH oxidases such as p38 MAPK and NFκB. Furthermore, previous studies have reported a requirement of p38 MAPK and NFκB activation in the increased CX<sub>3</sub>CL1 expression<sup>23–27</sup> and here we show through the blockade of p38 MAPK and NFκB signalling by pharmacological inhibition that CSE-induced activation of these signalling pathways is indispensable for endothelial CX<sub>3</sub>CL1 expression and its leukocyte-capturing function. Based on the evidence that the transcriptional activity of NFκB is regulated among others by p38 MAPK pathways,<sup>28</sup> it is likely that this kinase acts upstream of NFκB activation. Additionally, the human CX<sub>3</sub>CL1 promoter contains a number of putative DNA binding elements, including ones for NFκB.<sup>29</sup>

To determine if these results have any clinical relevance we examined mononuclear cells from patients with COPD. Our data demonstrated CX<sub>3</sub>CR1 overexpression and increased circulating numbers of CX<sub>3</sub>CR1<sup>+</sup> monocytes and lymphocytes in patients with COPD compared with those from their age-matched controls. Consequently, leukocyte adhesion to CSE-stimulated HUAECs was more pronounced in the COPD

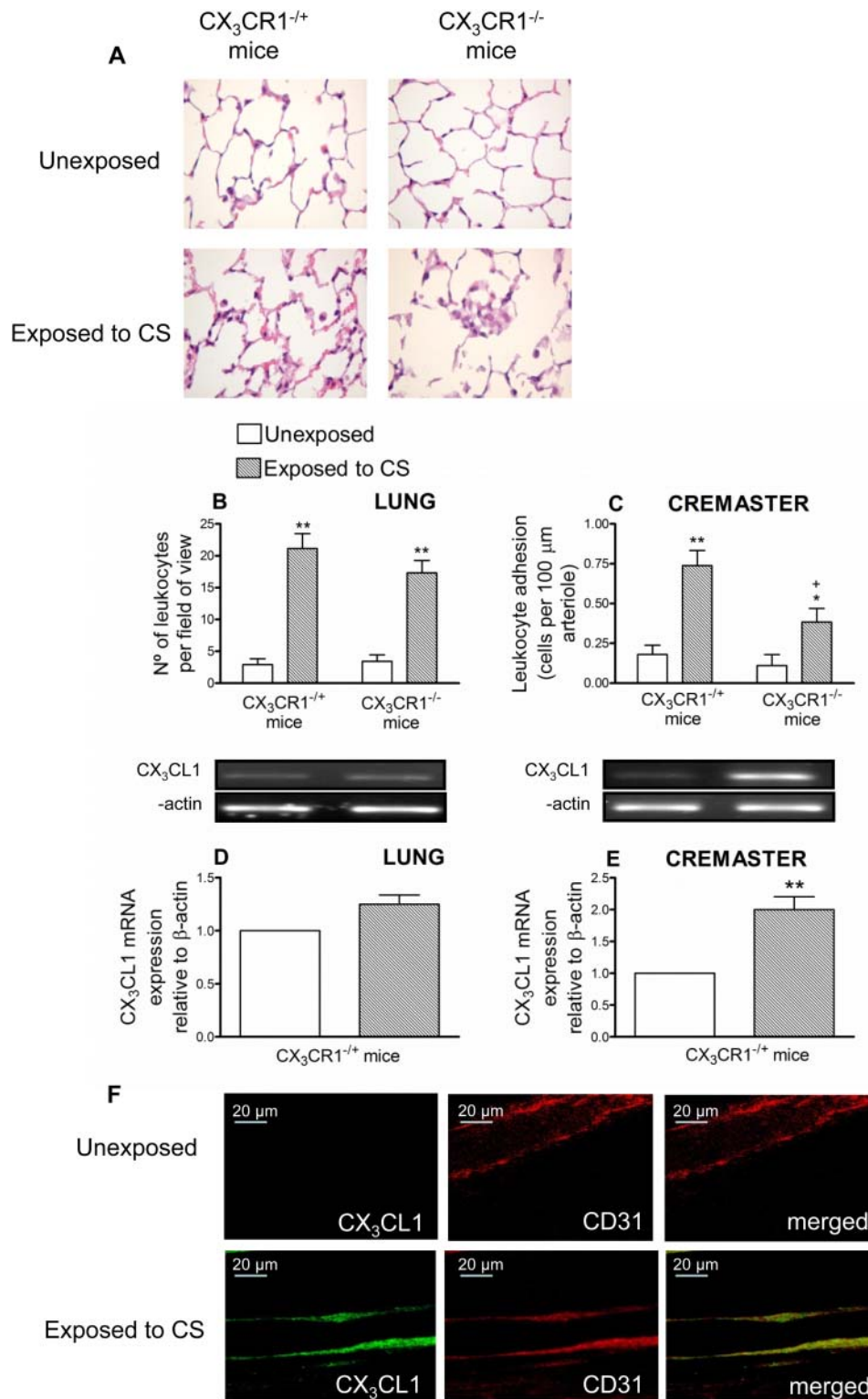


**Figure 6** Cigarette smoke (CS) exposure induces lung inflammation (A and B), leukocyte–arteriolar endothelial cell interactions (C) and increased CX<sub>3</sub>CL1 mRNA (D and E) and protein expression (E) in the mouse cremasteric microcirculation of CX<sub>3</sub>CR1-expressing (CX<sub>3</sub>CR1<sup>+/-</sup>) and CX<sub>3</sub>CR1-deficient (CX<sub>3</sub>CR1<sup>-/-</sup>) mice. Mice were exposed or left unexposed to CS for 3 days and responses examined 16 h later. Lungs were collected 16 h later and fixed for staining with hematoxylin/eosin (A) and cell counts were obtained (B). Leukocyte–arterial endothelium interactions were also determined (C). Results are mean ± SEM of n = 6–8 animals per group. \*p < 0.05 or \*\*p < 0.01 relative to no exposed animals; +p < 0.05 relative to CX<sub>3</sub>CR1<sup>+/-</sup> mice. Columns show the fold increase in lung (D) and cremaster (E) CX<sub>3</sub>CL1 mRNA expression relative to control β actin. Results are mean ± SEM of n = 4 independent experiments. \*\*p < 0.01 relative to no exposed animals. Some cremaster muscles were fixed for CX<sub>3</sub>CL1 and endothelium (CD31) staining (F). CX<sub>3</sub>CL1 expression is shown in green (stained with an Alexa Fluor 488-conjugated donkey anti-rabbit secondary antibody) and vessel endothelium (red) was stained with a PE-conjugated anti-mouse CD31 monoclonal antibody. Overlapping expression of CX<sub>3</sub>CL1 and CD31 is shown in yellow. Results are representative of n = 5–6 animals per group.

group. Moreover, although CX<sub>3</sub>CL1 neutralisation reduced the adhesion of CX<sub>3</sub>CR1<sup>+</sup> cells to the arterial endothelium in both groups, this effect was more marked when whole blood was from patients with COPD (52% vs 84% inhibition). Several explanations may account for the clinical impact of these results. First, an identified mutant form of the CX<sub>3</sub>CL1 receptor, termed CX<sub>3</sub>CR1-M280, is defective in mediating adhesive and chemotactic activity.<sup>30 31</sup> This mutated form of CX<sub>3</sub>CR1 is linked to lower risk of atherosclerosis, acute coronary events and coronary artery endothelial cell dysfunction.<sup>30 31</sup> Second, CX<sub>3</sub>CR1 upregulation was detected in circulating monocytes of patients with coronary artery disease.<sup>32</sup> Therefore, it is feasible that increased CX<sub>3</sub>CR1 expression/function in circulating mononuclear cells may establish a direct link between COPD and the development of cardiovascular disorders.

These striking observations prompted us to evaluate in vivo the impact of CS exposure. In our study CS exposure resulted in a moderated lung inflammation characterised by leukocyte infiltration in the lung tissue. However, no differences between both strains of animals (CX<sub>3</sub>CR1 expressing vs CX<sub>3</sub>CR1 deficient) were detected. This is not surprising given that neutrophils were the primary leukocytes involved in these responses and they do not express CX<sub>3</sub>CR1 receptor.<sup>21</sup> Likely a chronic exposure to this stimulus is required for the accumulation of CX<sub>3</sub>CR1<sup>+</sup> cells within the lung parenchyma as found in the past<sup>33</sup> since in our acute model no significant increase in lung CX<sub>3</sub>CL1 mRNA expression was detected. Previous reports have indicated that even moderate cigarette smoking leads to circulating monocyte activation and their increased adhesion to the endothelium.<sup>34</sup> Here we showed that CS-induced increased CX<sub>3</sub>CL1 expression is relevant for the attachment of mononuclear cells to the arterial endothelium. Unlike human monocytes, murine monocytes are the main subtype of leukocytes expressing CX<sub>3</sub>CR1.<sup>35</sup> Monocytes with high CX<sub>3</sub>CR1 expression were found to patrol blood vessels and extravasate rapidly in response to damage or infection as part of the early inflammatory response.<sup>35</sup> Furthermore, monocytes are abundant in atherosclerotic lesions and CX<sub>3</sub>CR1 has been implicated in the pathogenesis of this inflammatory disease.<sup>11 12</sup> Thus, it seems that acute exposure to CS causes endothelial dysfunction in the lung manifested as neutrophil infiltration and leukocyte-endothelial cell interactions in organs distant from the lung, resulting in CX<sub>3</sub>CL1-dependent arteriolar monocyte adhesion.

In conclusion, we have provided evidence that CS induces CX<sub>3</sub>CL1-dependent mononuclear cell arrest by arterial endothelium in vitro and in vivo. To our knowledge, this is the first report showing a previously undescribed mechanism that may account for the increased development of cardiovascular disorders in smokers. Our study also provides new insights into potential cellular and molecular mechanisms underlying these responses. Furthermore, we have proved the potential clinical implications of our findings since blockade of the CX<sub>3</sub>CL1/CX<sub>3</sub>CR1 axis dramatically reduced the adherence of mononuclear leukocytes from patients with COPD to CSE-stimulated arterial endothelium. Therefore, CX<sub>3</sub>CL1 and CX<sub>3</sub>CR1, and chemokine-regulatory factors such as TNF $\alpha$  may be considered as potential drug targets for the prevention and treatment of COPD-associated cardiovascular disease.

**Contributors** CR, CC, LP, MCN, CG, ES, EM and MJS participated in the acquisition of the data, and the analysis and interpretation of the results. AL contributed with vital reagents and was involved in the design of the study and in its revision prior to submission. EM was also involved in the design of the study and in its revision prior to submission. MJS was involved in the conception, hypothesis

delineation and design of the study as well as in the article writing. CR and CC contributed equally.

**Funding** This study was supported by grants SAF2008-03477, SAF2009-08913, SAF2011-23777, CP07/00179 and PI081875, Spanish Ministry of Science and Innovation, RIER RD08/0075/0016, Carlos III Health Institute, Spanish Ministry of Health, the European Regional Development Fund (FEDER) and research grants from Generalitat Valenciana (PROMETEO/2008/045; AP-055/08; GVACOMP2010-129). CC and CR were supported by a grant from the Spanish Ministry of Science and Innovation.

**Competing interests** None.

**Patient consent** Obtained.

**Ethics approval** Institutional ethics committee at the University Clinic Hospital of Valencia, Spain.

**Provenance and peer review** Not commissioned; externally peer reviewed.

## REFERENCES

- Sinden NJ, Stockley RA. Systemic inflammation and comorbidity in COPD: a result of 'overspill' of inflammatory mediators from the lungs? Review of the evidence. *Thorax* 2010;65:930–6.
- Forsdahl SH, Singh K, Solberg S, *et al.* Risk factors for abdominal aortic aneurysms: a 7-year prospective study: the Tromso Study, 1994–2001. *Circulation* 2009;119:2202–8.
- Ross R. The pathogenesis of atherosclerosis: a perspective for the 1990s. *Nature* 1993;362:801–9.
- Landmesser U, Hornig B, Drexler H. Endothelial function: a critical determinant in atherosclerosis? *Circulation* 2004;109:1127–33.
- Newby DE, Wright RA, Labinjoh C, *et al.* Endothelial dysfunction, impaired endogenous fibrinolysis, and cigarette smoking: a mechanism for arterial thrombosis and myocardial infarction. *Circulation* 1999;99:1411–15.
- Lang NN, Gudmundsdottir IJ, Boon NA, *et al.* Marked impairment of protease-activated receptor type 1-mediated vasodilation and fibrinolysis in cigarette smokers: smoking, thrombin, and vascular responses in vivo. *J Am Coll Cardiol* 2008;52:33–9.
- Ley K, Laudanna C, Cybulsky MI, *et al.* Getting to the site of inflammation: the leukocyte adhesion cascade updated. *Nat Rev Immunol* 2007;7:678–89.
- Baggiolini M. Chemokines in pathology and medicine. *J Intern Med* 2001;250:91–104.
- Ludwig A, Weber C. Transmembrane chemokines: versatile 'special agents' in vascular inflammation. *Thromb Haemostasis* 2007;97:694–703.
- Beck G, Ludwig F, Schulte J, *et al.* Fractalkine is not a major chemoattractant for the migration of neutrophils across microvascular endothelium. *Scand J Immunol* 2003;58:180–7.
- Lesnik P, Haskell CA, Charo IF. Decreased atherosclerosis in CX3CR1<sup>-/-</sup> mice reveals a role for fractalkine in atherogenesis. *J Clin Invest* 2003;111:333–40.
- Combadiere C, Potteaux S, Gao JL, *et al.* Decreased atherosclerotic lesion formation in CX3CR1/apolipoprotein E double knockout mice. *Circulation* 2003;107:1009–16.
- Edirisinghe I, Yang SR, Yao H, *et al.* VEGFR-2 inhibition augments cigarette smoke-induced oxidative stress and inflammatory responses leading to endothelial dysfunction. *FASEB J* 2008;22:2297–310.
- Doz E, Noulin N, Boichot E, *et al.* Cigarette smoke-induced pulmonary inflammation is TLR4/MyD88 and IL-1R1/MyD88 signaling dependent. *J Immunol* 2008;180:1169–78.
- Su Y, Han W, Giraldo C, *et al.* Effect of cigarette smoke extract on nitric oxide synthase in pulmonary artery endothelial cells. *Am J Respir Cell Mol Biol* 1998;19:819–25.
- Orosz Z, Csiszar A, Labinsky N, *et al.* Cigarette smoke-induced proinflammatory alterations in the endothelial phenotype: role of NAD(P)H oxidase activation. *Am J Physiol Heart Circ Physiol* 2007;292:H130–9.
- Pendyala S, Usatyuk PV, Gorshkova IA, *et al.* Regulation of NADPH oxidase in vascular endothelium: the role of phospholipases, protein kinases, and cytoskeletal proteins. *Antioxid Redox Signal* 2009;11:841–60.
- BelAiba RS, Djordjevic T, Petry A, *et al.* NOX5 variants are functionally active in endothelial cells. *Free Radic Biol Med* 2007;42:446–59.
- Petrescu F, Voican SC, Silosi I. Tumor necrosis factor- $\alpha$  serum levels in healthy smokers and nonsmokers. *Int J Chron Obstruct Pulmon Dis* 2010;5:217–22.
- Mossman BT, Lounsbury KM, Reddy SP. Oxidants and signaling by mitogen-activated protein kinases in lung epithelium. *Am J Respir Cell Mol Biol* 2006;34:666–9.
- Imai T, Hieshima K, Haskell C, *et al.* Identification and molecular characterization of fractalkine receptor CX3CR1, which mediates both leukocyte migration and adhesion. *Cell* 1997;91:521–30.
- Michaud SE, Dussault S, Groleau J, *et al.* Cigarette smoke exposure impairs VEGF-induced endothelial cell migration: role of NO and reactive oxygen species. *J Mol Cell Cardiol* 2006;41:275–84.

- 23 Chandrasekar B, Mummidhi S, Perla RP, *et al.* Fractalkine (CX3CL1) stimulated by nuclear factor kappaB (NF-kappaB)-dependent inflammatory signals induces aortic smooth muscle cell proliferation through an autocrine pathway. *Biochem J* 2003;373:547–58.
- 24 Montezano AC, Burger D, Paravicini TM, *et al.* Nicotinamide adenine dinucleotide phosphate reduced oxidase 5 (Nox5) regulation by angiotensin II and endothelin-1 is mediated via calcium/calmodulin-dependent, rac-1-independent pathways in human endothelial cells. *Circ Res* 2010;106:1363–73.
- 25 Alvarez A, Sanz MJ. Reactive oxygen species mediate angiotensin II-induced leukocyte–endothelial cell interactions in vivo. *J Leukoc Biol* 2001;70:199–206.
- 26 Mateo T, Naim Abu Nabah Y, Losada M, *et al.* A critical role for TNFalpha in the selective attachment of mononuclear leukocytes to angiotensin-II-stimulated arterioles. *Blood* 2007;110:1895–902.
- 27 Matsumiya T, Ota K, Imaizumi T, *et al.* Characterization of synergistic induction of CX3CL1/fractalkine by TNF-alpha and IFN-gamma in vascular endothelial cells: an essential role for TNF-alpha in post-transcriptional regulation of CX3CL1. *J Immunol* 2010;184:4205–14.
- 28 Vanden Berghe W, Plaisance S, Boone E, *et al.* p38 and extracellular signal-regulated kinase mitogen-activated protein kinase pathways are required for nuclear factor-kappaB p65 transactivation mediated by tumor necrosis factor. *J Biol Chem* 1998;273:3285–90.
- 29 Bhavsar PK, Sukkar MB, Khorasani N, *et al.* Glucocorticoid suppression of CX3CL1 (fractalkine) by reduced gene promoter recruitment of NF-kappaB. *FASEB J* 2008;22:1807–16.
- 30 McDermott DH, Halcox JP, Schenke WH, *et al.* Association between polymorphism in the chemokine receptor CX3CR1 and coronary vascular endothelial dysfunction and atherosclerosis. *Circ Res* 2001;89:401–7.
- 31 McDermott DH, Fong AM, Yang Q, *et al.* Chemokine receptor mutant CX3CR1-M280 has impaired adhesive function and correlates with protection from cardiovascular disease in humans. *J Clin Invest* 2003;111:1241–50.
- 32 Apostolakis S, Krambovitis E, Vlata Z, *et al.* CX3CR1 receptor is up-regulated in monocytes of coronary artery diseased patients: impact of pre-inflammatory stimuli and renin–angiotensin system modulators. *Thromb Res* 2007;121:387–95.
- 33 McComb JG, Ranganathan M, Liu XH, *et al.* CX3CL1 up-regulation is associated with recruitment of CX3CR1+ mononuclear phagocytes and T lymphocytes in the lungs during cigarette smoke-induced emphysema. *Am J Pathol* 2008;173:949–61.
- 34 Bergmann S, Siekmeier R, Mix C, *et al.* Even moderate cigarette smoking influences the pattern of circulating monocytes and the concentration of sICAM-1. *Respir Physiol* 1998;114:269–75.
- 35 Auffray C, Fogg D, Garfa M, *et al.* Monitoring of blood vessels and tissues by a population of monocytes with patrolling behavior. *Science* 2007;317:666–70.

## **SUPPLEMENTAL MATERIAL**

### **Cell Culture**

Human umbilical arterial endothelial cells (HUAEC) were isolated by collagenase treatment [1] and maintained in human endothelial cell specific medium (EBM-2) supplemented with endothelial growth media (EGM-2) and 10% FCS. Cells up to passage 1 were grown to confluence to preserve endothelial features. Prior to every experiment, cells were incubated 16 h in medium containing 1% FCS. Previous studies carried out by our group have shown that human umbilical vein endothelial cells (HUVEC) do not behave like HUAEC in response to relevant cardiovascular stimuli such as angiotensin II [2,3]. In this context, HUAEC and HUVEC showed dissimilar mononuclear cell and neutrophil adhesion when the same stimulus was applied.

### **Cigarette smoke extract (CSE) preparation**

The composition of 3R4 research grade cigarettes was as follows: total particulate matter, 10.9 mg/cigarette; tar, 9.5 mg/cigarette; and nicotine, 0.726 mg/cigarette. 10% CSE was prepared by bubbling smoke from one cigarette 3R4F into 10 ml of EGM-2 culture media without FBS at a rate of 1 cigarette / 2 min. The pH of the CSE was adjusted to 7.4 and sterile filtered through a 0.22  $\mu$ m filter. CSE preparation was standardized by measuring the absorbance (optical density=  $0.86 \pm 0.05$ ) at a wavelength of 320 nm. The pattern of absorbance (spectrogram) observed at  $\lambda$ 320 showed very little variation between different preparations of CSE. CSE was freshly prepared for each experiment and diluted with culture media supplemented with 0.1% FBS immediately before use. Control medium was prepared by bubbling air through 10 ml of culture media without FBS, the pH was adjusted to 7.4, and the

medium was sterile filtered as described above. In initial experiments, a range of concentrations of CSE were tested (0.1-3%). Based on these preliminary studies a final concentration of 1% was used in all subsequent experiments.

### **RT-PCR**

The reverse transcription was performed in 300 ng of total RNA with TaqMan reverse transcription reagents kit. cDNA was amplified with specific primers for fractalkine (CX<sub>3</sub>CL1), TNF $\alpha$ , Nox2, Nox4, Nox5 and GAPDH (all pre-designed by Applied Biosystems, Carlsbad, CA) in a 7900HT Fast Real-Time PCR System (Applied Biosystem) using Universal Master Mix (Applied Biosystems). Relative quantification of these different transcripts was determined with the  $2^{-\Delta\Delta C_t}$  method using GAPDH as endogenous control and normalized to control group.

### **Flow cytometry**

The cells were washed and incubated at  $2 \times 10^6$  cells/ml with a PE-conjugated mAb against human CX<sub>3</sub>CL1 (1.25  $\mu$ g/ml) in PBS with 0.2% BSA and 0.05% NaN<sub>3</sub> for 1 h on ice. After 2 washes, cells were suspended in PBS containing 2% paraformaldehyde. The fluorescence signal of the labeled cells was then analyzed by flow cytometry (FACSCanto Flow cytometer, BD Biosciences, Franklin Lakes, NJ). The expression of CX<sub>3</sub>CL1 (PE-fluorescence) was expressed as the mean of fluorescence intensity (MFI).

### **Leukocyte-endothelial cell interactions under flow conditions**

Human mononuclear cells were obtained from buffy coats of healthy donors by Ficoll Hypaque density gradient centrifugation [1]. The Glycotech flow chamber was assembled and placed onto an inverted microscope stage, and then freshly isolated mononuclear cells ( $1 \times 10^6$ /ml) were perfused across the endothelial monolayers. In all experiments, leukocyte interactions were determined after 5 min at 0.5 dyn/cm<sup>2</sup>. Cells

interacting on the surface of the endothelium were visualized and recorded ( $\times 20$  objective,  $\times 10$  eyepiece) using phase-contrast microscopy (Axio Observer A1 Carl Zeiss microscope, Thornwood, NY).

### **Immunofluorescence**

Confluent endothelial cells were grown on glass coverslips and stimulated with 1% CSE or vehicle for 24 h. The cells were fixed with 4% paraformaldehyde, and blocked in a PBS solution containing 1% BSA. Then, they were incubated at 4°C overnight with a primary mouse mAb against human CX<sub>3</sub>CL1 (1:200 dilution) in a 0.1% BSA/PBS solution, followed by incubation with a secondary antibody Alexa Fluor 488-conjugated goat anti-mouse mAb (1/1000 dilution) at room temperature for 45 min. Cell nuclei were counterstained with 4'-6-diamidino-2-phenylindole (DAPI). Images were captured with a confocal microscope (Leica TCS/SP2, Solms, Germany).

### ***Western Blot.***

After treatment, cells were washed, detached, collected, and centrifuged at 15,000 g at 4°C for 30 min to yield the whole extract. Protein content was determined by the Bradford method. Samples were denatured, subjected to SDS-PAGE using a 10% running gel, and transferred to nitrocellulose membrane. Nonspecific binding sites were blocked with 3% BSA in TBS solution, and were then incubated overnight with rabbit polyclonal antibody against human CX<sub>3</sub>CL1 (0.2  $\mu$ g/ml), a mouse polyclonal antibody against human Nox2 (0.2  $\mu$ g/ml), a rabbit polyclonal antibody against human Nox4 (2  $\mu$ g/ml), a rabbit polyclonal antibody against human Nox5 (2  $\mu$ g/ml) or a goat polyclonal anti-human TNF $\alpha$  (0.1  $\mu$ g/ml). Then they were washed and further incubated for 1 h with the corresponding secondary HRP-linked antibody: anti-rabbit IgG (1:2000 dilution), anti-goat IgG or anti-mouse IgG (1:2000 dilution) and developed using the ECL procedure. Signals were recorded using a luminiscent

analyser (FujiFilm image Reader LAS1000, Fuji, Tokyo, Japan) and analyzed using the software ImageJ (Windows free version).

### **Transfection of TNF $\alpha$ , Nox2, Nox4 or Nox5 siRNA**

The transfection reagent used was Lipofectamine RNAiMAX, following the manufacturer's instructions. The mRNA expression for transcripts was determined by real time RT-PCR after 48 h post-silencing and compared with siRNA control at the respective time to determine silencing efficiency. Cells were also tested for TNF $\alpha$ , Nox2, Nox4 or Nox5 expression by western blot of cells lysates. In addition, cell viability after control or siRNA transfection was assessed by MTT assay. Cells were 94-97% viable.

### **Experimental protocols**

In a first set of experiments, HUAEC were grown to confluence and stimulated with 0.1-3% CSE or TNF $\alpha$  (20 ng/ml) for 1, 4 or 24 and CX<sub>3</sub>CL1 mRNA expression was determined by RT-PCR and protein expression by flow cytometry, immunofluorescence analysis and western blot.

In another group, HUAEC were stimulated with with 1% CSE for 24 h. Freshly isolated human mononuclear cells were perfused across the endothelial cell monolayers and leukocyte-endothelial interactions were determined under flow conditions. To determine the effect of endothelial CX<sub>3</sub>CL1 expression on mononuclear recruitment, endothelial cells were incubated with a monoclonal neutralizing antibody against human CX<sub>3</sub>CL1 (5  $\mu$ g/ml) or with an isotype matched control antibody (MOPC-21, 5  $\mu$ g/ml) 10 min prior to mononuclear cell superfusion.

To evaluate the potential involvement of NADPH and xanthine oxidase (XO) on CSE-induced responses, cells were incubated for 1 h with a NADPH oxidase inhibitor

(apocynin, 30  $\mu$ M) or with a XO inhibitor (allopurinol, 100  $\mu$ M) and then stimulated with 1% CSE for 24 h. The doses of these compounds were used as previously described.[4] and, no direct toxicity was found by MTT assay (viability 95-98%). Since, the NADPH oxidase isoforms Nox2, Nox4, and Nox5 are all expressed in endothelial cells,[5,6] in subsequent experiments, HUAEC were transfected with either control or Nox2, Nox4 or Nox5-specific siRNA. Forty eight h post-transfection they were stimulated with 1 % CSE and CX<sub>3</sub>CL1 expression and mononuclear cell arrest evaluated.

To investigate the possible contribution of TNF $\alpha$  to CSE-induced CX<sub>3</sub>CL1 expression and mononuclear cells recruitment, we first incubated the cells with 1% CSE for 24 h and TNF $\alpha$  expression was determined by western blot. Next, HUAEC were transfected for 48 h with control or TNF- $\alpha$ -specific siRNA before CSE stimulation and CSE-induced responses were measured 24 h later.

To extend these findings, in additional experiments, the phosphorylation/activation of p38MAPK and NF $\kappa$ B were determined by flow cytometry as previously described.[3] HUAEC were stimulated or not with 1% CSE for 30 – 60 min. The endothelial cells were then fixed and permeabilized with BD Cytotfix/Cytoperm solution and sequentially stained with a Alexa Fluor-conjugated mouse anti-human p38MAPK (pT80/pY182) and with a PE-conjugated mouse anti-human p65 subunit (pS529) mAbs.

To further elucidate the signalling pathways involved in CSE-induced responses, endothelial cells were pretreated with the inhibitors of p38MAPK (SB202190, 20  $\mu$ M) or NF $\kappa$ B (MOL294, 2.5  $\mu$ M) 1 h before CSE stimulation. These concentrations have previously been employed to inhibit p38MAPK and NF $\kappa$ B.[7,8] and, cell viability by MTT assay was higher than 95%. After 24 h stimulation with 1% CSE, both CX<sub>3</sub>CL1 expression and mononuclear cell arrest were determined.

### **Studies in COPD patients and age-matched controls**

A total of 52 subjects (29 COPD patients and 23 control age-matched subjects without COPD) were included in this study. COPD patients and control subjects were recruited by the Pneumology Unit of University Clinic Hospital of Valencia, Valencia, Spain. All patients had COPD confirmed by medical history, clinical and functional examinations according to criteria established by the American Thoracic Society (Standards of diagnosis and care of patients with chronic obstructive pulmonary disease. Am J Respir Crit Care Med 1995;152 (Suppl):77-120): smoking history of  $\geq 10$  pack-year, the post-bronchodilator ratio of low forced expiratory volume in 1 second ( $FEV_1$ ) and forced vital capacity (FVC),  $FEV_1/FVC$  ratio was  $< 0.70$  and the post-bronchodilator  $FEV_1$  was  $< 80\%$ . One pack-year was defined as smoking 20 cigarettes per day for one year. The control group was volunteers seen at the respiratory function laboratory for routine preoperative assessment. They had no history of pulmonary disease or respiratory symptoms, and had a normal spirometry. In order to study homogeneous samples of both COPD patients and controls, only subjects older than 60 years of age were included. Written informed consent was obtained from all volunteers. Spirometry was performed on a Master Scope (Jaeger, Germany), after inhalation of 0.4 mg of salbutamol. A minimum of three airflow and volume tracings were obtained and the highest value for  $FEV_1$  and FVC as percent predicted normal were used for calculations. Most of the patients used in this study presented moderate COPD according with the criteria of GOLD classification (Global Initiative for Chronic Obstructive Lung Disease. Global strategy for the diagnosis, management, and prevention of COPD. [December, 2011]. Available from: <http://www.goldcopd.org>). In this regard, 8% were GOLD1 (mild), 60% were GOLD2 (moderate), 28% were GOLD3 (severe) and 4% were GOLD4 (very severe). Clinical features of patients and age-matched controls are shown in Table 1.

Table 1: Patient demographics of the subjects studied (data expressed as mean  $\pm$  SEM)

	Control non smoker volunteers	COPD subjects
Numbers per group (n)	23	29
Smoking (pack-years)	none	49.1 $\pm$ 7.07
Age	69.48 $\pm$ 1.79	68.52 $\pm$ 1.88
FEV <sub>1</sub> (% Predicted)	94.23 $\pm$ 3.95	59.32 $\pm$ 3.54**
FEV <sub>1</sub> /FVC (%)	74.85 $\pm$ 1.40	57.84 $\pm$ 2.03**
Gender (M)	100%	100%

Pack-year (n° cigarettes per day per smoking years / 20). FEV<sub>1</sub> % Predicted, forced expiratory volume in 1 s (%); FVC, forced vital capacity. \*\*p<0.01 relative to values in the control group.

To determine the expression of CX<sub>3</sub>CL1 receptor (CX<sub>3</sub>CR1) on circulating monocytes and lymphocytes from COPD patients and control-matched individuals, a flow cytometry analysis was employed. Duplicate samples (100  $\mu$ l) of heparinized whole blood were incubated on ice in the dark for 20 min with saturated amounts (10  $\mu$ l) of the carboxyfluorescein (CFS)-conjugated mAb against human CX<sub>3</sub>CR1. RBCs were lysed and leukocytes were fixed using an automated EPICS Q-PREP system (Coulter Electronics, Hialeah, Florida). Samples were run in a Flow cytometer (FACSCanto Flow cytometer, BD Biosciences, Franklin Lakes, NJ). The expression of CX<sub>3</sub>CR1 (CFS fluorescence) was measured on monocytes and lymphocytes by their specific features of size (forward scatter) and granularity (side scatter) and expressed as the mean of fluorescence intensity (MFI) as it is illustrated in Figure II (online supplemental data 2).

In another set experiments, a dynamic flow chamber assay was performed using heparinized whole blood from both groups under investigation. Diluted whole blood (1/10 in HBSS) of COPD patients and control-matched subjects was perfused across unstimulated or 1% CSE-stimulated endothelial monolayers as previously described and leukocyte-endothelial cell interactions were determined. Some plates were incubated with a monoclonal neutralizing antibody against human CX<sub>3</sub>CL1 (5 µg/ml) or with an isotype matched control antibody (MOPC-21, 5 µg/ml) 10 min before blood perfusion.

Finally, heparinized human whole blood (10 U heparin/ml) from COPD patients and healthy control-matched volunteers was collected. Before centrifugation to obtain plasma, further heparin was added to the blood sample (to 100 U/ml). This procedure was used to help to dissociate chemokines from blood cells. Plasma samples were stored at -80°C. Human CX<sub>3</sub>CL1 was measured in plasma by ELISA, as previously described.[9] Results are expressed as pM chemokine in the supernatant.

### **Animals**

The investigation conforms with the Guide for the Care and Use of Laboratory Animals published by the US National Institutes of Health and was approved by the ethics review board of the Faculty of Medicine, University of Valencia.

Male mice of C57BL/6 background carrying targeted knock in of GFP to disrupt the CX<sub>3</sub>CR1 gene have been used in numerous studies[10] in which male CX<sub>3</sub>CR1<sup>gfp/+</sup> mice were used as heterozygote controls (CX<sub>3</sub>CR1<sup>-/+</sup>) and homozygote CX<sub>3</sub>CR1<sup>gfp/gfp</sup> animals that do not express CX<sub>3</sub>CR1 receptor as CX<sub>3</sub>CR1 deficient mice (CX<sub>3</sub>CR1<sup>-/-</sup>). Animal colonies were bred and maintained under specific pathogen-free conditions. For all the experimental period the mice were fed with autoclaved balanced diet and water. The animals used were 22–30 g weight.

### **Cigarette smoke exposure**

Mice were placed in a plexiglass chamber (volume of 20 l) covered by a disposable filter. The smoke produced by cigarette burning was introduced at a rate of 25 ml/min into the chamber with the continuous airflow generated by a mechanical ventilator, with no influence on the chamber temperature (<0.1°C variation). The animals received smoke from 5 research grade cigarettes (3R4F) per exposure, 2 exposures a day during 3 days. Experiments were carried out 16 h after the last exposure.

### **Intravital microscopy**

The mouse cremaster preparation used in this study was similar to that described previously.[11] Mice were anesthetized by i.p. injection with a mixture of xylazine hydrochloride (10 mg/kg) and ketamine hydrochloride (200 mg/kg). Additional anesthetic (30 µl, i.v.) was administered as required to maintain profound anesthesia. A polyethylene catheter was placed in the jugular vein to permit the intravenous administration of additional anesthetic. The cremaster muscle was dissected free of tissues and exteriorized onto an optical clear viewing pedestal. The muscle was cut longitudinally with a cautery and held flat against the pedestal by attaching silk sutures to the corners of the tissue. The muscle was then perfused continuously at a rate of 1 ml/min with warmed bicarbonate-buffered saline (pH 7.4).

The cremasteric microcirculation was then observed using an intravital microscope (Nikon Optiphot-2, SMZ1, Badhoevedorp, Netherlands) equipped with a 50x objective lens (Nikon SLDW, Badhoevedorp, The Netherlands) and a 10x eyepiece. A video camera (Sony SSC-C350P, Koeln, Germany) mounted on the microscope projected the image onto a color monitor and the images were CCD recorded for playback analysis. Cremasteric arterioles (20-40 µm in diameter) were selected for study. Vessel diameter

was measured on-line by using a video caliper (Microcirculation Research Institute, Texas A&M University, College Station, Texas).

The number of adherent leukocytes was determined off-line during playback of the recorded images. A leukocyte was defined as adherent to arteriolar endothelium, if it was stationary for at least 30 s. Leukocyte adhesion was expressed as the number per 100  $\mu\text{m}$  length of vessel per 5 min. In each animal, leukocyte responses were averaged in three to five randomly selected arterioles.

### **RT-PCR**

Real time RT-PCR was performed using standard protocols employing the following primers: mouse CX<sub>3</sub>CL1 forward, 5'-GGACAGGACCTCAGTCCAGA- 3', reverse 5'-TCGGGGACAGGAGTGATAAG -3', (256 bp product).  $\beta$ -actin forward, 5'-GTGGGCCGCTCTAGGCACCAA-3', reverse 5'-CTCTTTGATGTCACGCACGATTTC-3'(539 bp product). The PCR products were analyzed by 1.5% agarose gel electrophoresis and visualized by ethidium bromide staining. CX<sub>3</sub>CL1 mRNA abundance was determined by comparison with  $\beta$ -actin.

### **Histology and Immunofluorescence**

Immunofluorescence studies were performed following a similar protocol to that previously described. [12] Once intravital microscopy determinations were performed, mice were sacrificed and the cremaster muscle was isolated and fixed in 4 % paraformaldehyde for 10 minutes. Muscles were incubated in 0.2% Triton X-100, 1% BSA and 0.5% horse serum in phosphate-buffered saline (PBS) for 2 h. Then muscles were incubated overnight at 4°C with a primary Ab rabbit anti-mouse CX<sub>3</sub>CL1 (1/100 dilution) or eFluor 450-conjugated anti-mouse CD31 (PECAM-1) (1/100 dilution). Samples were then washed with PBS and incubated for 1.5 h at room temperature with Alexa Fluor 488-conjugated donkey anti-rabbit secondary antibody (1/500 dilution). All

antibodies were diluted in 0.1% PBS/BSA. Muscles were then mounted with Slowfade Gold Reagent (Invitrogen, Eugene, Oregon, USA). Images were acquired by using a fluorescence microscope (Axio Observer A1, Carl Zeiss, NY) equipped with a 40x objective lens and a 10x eyepiece.

In some animals, lungs were removed, fixed with 4% paraformaldehyde and embedded in paraffin. Sections (4  $\mu$ m-thick) were obtained and then stained with hematoxylin/eosin. Cells were counted in 10 different fields and averaged.

### **Materials**

Endothelial basal medium-2 (EBM-2) supplemented with endothelial growth medium-2 (EGM-2) were acquired from Lonza Iberica (Barcelona, Spain). Ketamine and xylazine hydrochloride were from ORION Pharma (Espoo, Finland). Apocynine, allopurinol, SB202190, Thiazolyl Blue Tetrazolium Bromide, the mouse anti-human  $\beta$ -actin mAb (clone AC-15), the mAb IgG1 (MOCPC21) and the rabbit polyclonal anti-human Nox 5 Ab were purchased from Sigma-Aldrich (Madrid, Spain). The rabbit polyclonal anti-mouse CX<sub>3</sub>CL1 and the PE-conjugated conjugated rat monoclonal anti-mouse CD31 (clone 390) were from eBioscience (Hatfield, UK). Recombinant human TNF $\alpha$  and the rabbit polyclonal anti-human CX<sub>3</sub>CL1 employed for western blotting were acquired from Peprotech (London, UK). The PE-conjugated mouse monoclonal anti-human CX<sub>3</sub>CL1 (clone 51637), the CFS-conjugated mouse monoclonal anti-human CX<sub>3</sub>CR1 (clone 528728), the mouse monoclonal anti-human CX<sub>3</sub>CL1 (clone 81506), the biotinylated mouse monoclonal anti-human CX<sub>3</sub>CL1 (clone 51637) and the goat polyclonal anti-human TNF $\alpha$  were purchased from R&D Systems (Abingdon, UK). The rabbit polyclonal anti-human Nox 4 was from Abcam (Cambridge, UK), and the mouse monoclonal anti-human Nox 2 (clone NL7) Ab was purchased to Serotec (Oxford, UK). The sodium heparin (5000 U/ml or 50 mg/ml)

was from Pharmaceutical Laboratories Rovi SA (Madrid, Spain). Neutravidin-HRP was supplied by Perbio Science (Northumberland, UK) and the K-Blue substrate by Neogen (Ayr, Scotland, UK). The cytotoxicity detection Kit plus LDH were obtained from Roche Applied science (Mannheim, Germany), Ficoll-Paque TM plus and ECL developer were purchased from GE Healthcare (Chalfont St Giles, UK). DAPI, TRIzol isolation reagent and Alexa Fluor 488-conjugated secondary antibodies were from Molecular Probes-Invitrogen (Carlsbad, CA). The secondary HRP-linked anti-rabbit IgG Ab was supplied by Cell Signalling Technology (Grand Island, NY). The secondary Abs, HRP-linked anti-goat IgG and HRP-linked anti-mouse IgG were purchased from Dako (Glostrup, Denmark). BD Cytfix/Cytoperm solution, PE-conjugated mouse anti-p65 (pS529) (clone K10-895.12.50) and the Alexa Fluor-conjugated mouse anti-p38MAPK (pT80/pY182) (clone 36/p38; pT180/pY182) were from BD Biosciences (San Jose, CA). TNF $\alpha$ , Nox2, Nox4 or Nox5-specific siRNA were purchased to Dharmacon (Lafayette, CO). TaqMan reverse transcription reagents kit were from Applied Biosystems, (Perkin-Elmer Corporation, Carlsbad, CA). MOL-294 was kindly donated by Dr. Kahn (Department of Pathobiology, University Washington, Seattle, WA).

### **Statistical Analysis**

Values were expressed as mean  $\pm$  SEM. Differences between two groups were determined by paired or unpaired Student's t test, as appropriate. Data within multiple groups were compared using an analysis of variance (one-way ANOVA) including a Newman-Keuls post hoc test for multiple comparisons. Data were considered statistically significant when  $p < 0.05$ .

### **References**

1. Mateo T, Naim Abu Nabah Y, Losada M, *et al.* A critical role for TNF $\alpha$  in the selective attachment of mononuclear leukocytes to angiotensin-II-stimulated arterioles. *Blood.* 2007;**110**:1895-1902.
2. Abu-Taha M, Rius C, Hermenegildo C, Noguera I, *et al.* Menopause and ovariectomy cause a low grade of systemic inflammation that may be prevented by chronic treatment with low doses of estrogen or losartan. *J Immunol.*2009;**183**:1393-1402.
3. Rius C, Abu-Taha M, Hermenegildo C, *et al.* Trans- but not cis-resveratrol impairs angiotensin-II-mediated vascular inflammation through inhibition of NF-kappaB activation and peroxisome proliferator-activated receptor-gamma upregulation. *J Immunol.*2010;**185**:3718-3727.
4. Beltran AE, Briones AM, Garcia-Redondo AB, *et al.* p38 MAPK contributes to angiotensin II-induced COX-2 expression in aortic fibroblasts from normotensive and hypertensive rats. *J Hypertens.* 2009;**27**:142-154.
5. BelAiba RS, Djordjevic T, Petry A, *et al.* NOX5 variants are functionally active in endothelial cells. *Free Radic Biol Med.* 2007;**42**:446-459.
6. Pendyala S, Gorshkova IA, Usatyuk PV, *et al.* Role of Nox4 and Nox2 in hyperoxia-induced reactive oxygen species generation and migration of human lung endothelial cells. *Antioxid Redox Signal.* 2009;**11**:747-764.
7. Goebeler M, Kilian K, Gillitzer R, *et al.* The MKK6/p38 stress kinase cascade is critical for tumor necrosis factor-alpha-induced expression of monocyte-chemoattractant protein-1 in endothelial cells. *Blood.* 1999;**93**:857-865.
8. Henderson WR, Jr., Chi EY, Teo JL, *et al.* A small molecule inhibitor of redox-regulated NF-kappa B and activator protein-1 transcription blocks allergic

airway inflammation in a mouse asthma model. *J Immunol.* 2002;**169**:5294-5299.

- 9.** Mateo T, Abu Nabah YN, Abu Taha M, *et al.* Angiotensin II-induced mononuclear leukocyte interactions with arteriolar and venular endothelium are mediated by the release of different CC chemokines. *J Immunol.* 2006;**176**:5577-5586.
- 10.** Jung S, Aliberti J, Graemmel P, *et al.* Analysis of fractalkine receptor CX(3)CR1 function by targeted deletion and green fluorescent protein reporter gene insertion. *Mol Cell Biol.* 2000;**20**:4106-4114.
- 11.** Company C, Piqueras L, Naim Abu Nabah Y, *et al.* Contributions of ACE and mast cell chymase to endogenous angiotensin II generation and leucocyte recruitment in vivo. *Cardiovasc Res.* 2011;**92**:48-56.
- 12.** Massena S, Christoffersson G, Hjertstrom E, *et al.* A chemotactic gradient sequestered on endothelial heparan sulfate induces directional intraluminal crawling of neutrophils. *Blood.* 2010;**116**:1924-1931.

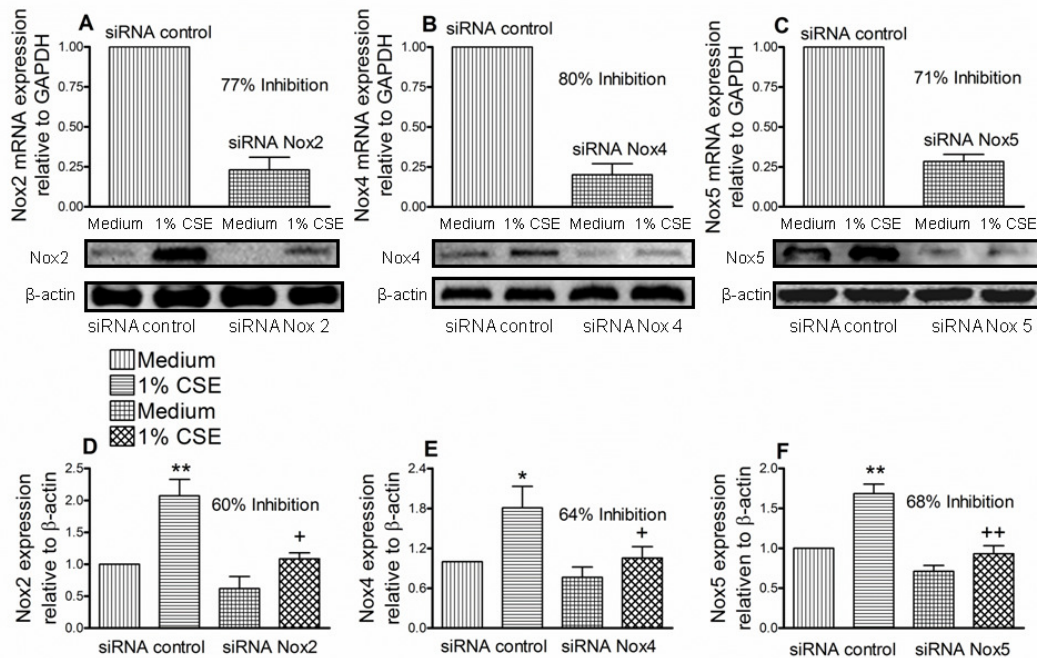


**Figure I: 1% CSE increases Nox2, Nox4 or Nox5 expression in HUAEC which is abolished in HUAEC transfected with siRNAs targeting Nox2, Nox4 or Nox5.** Endothelial cells were transfected with control siRNA or Nox2siRNA, Nox4siRNA or Nox5siRNA. 48h post-transfection cells were stimulated or not with 1% CSE for 24 h. Relative quantification of the mRNA levels of the different Nox isoforms and GAPDH was determined by real time quantitative RT-PCR by the comparative Ct method. Columns show the fold increase in the expression of Nox mRNA, relative to control values, calculated as the mean  $\pm$  SEM of the  $2^{-\Delta\Delta Ct}$  values of n= 4-5 independent experiments. Protein expression of the different Nox isoforms was determined by western blot. Results (mean  $\pm$  SEM of at least 4 independent experiments) are expressed as fold increase of the Nox isoform relative to  $\beta$ -actin. Representative gels are also shown. \* $p < 0.05$  or \*\* $p < 0.01$  relative to values in the control group; + $p < 0.05$  relative to the 1% CSE group.

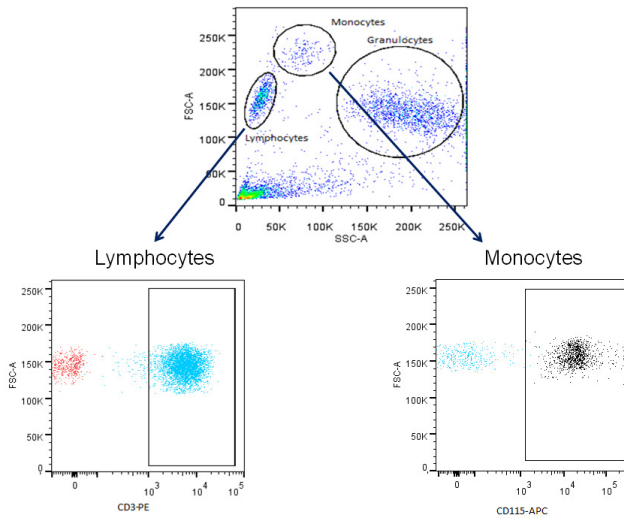


**Figure II: Flow-cytometry detection and morphologic gating of human monocytes and lymphocytes in whole blood.** In initial experiments lymphocytes were stained with a PE-labeled anti-CD3 mAb and monocytes with an APC-labeled anti-CD115 mAb. Once detected, they were gated based on their specific features of size (forward scatter) and granularity (side scatter).